Mice expressing a humanized form of VEGF-A may provide insights into the safety and efficacy of anti-VEGF antibodies

Hans-Peter Gerber*, Xiumin Wu, Lanlan Yu, Christian Wiesmann, Xiao Huan Liang, Chingwei V. Lee, Germaine Fuh, Christine Olsson, Lisa Damico, David Xie, Y. Gloria Meng, Johnny Gutierrez, Racquel Corpuz, Bing Li, Linda Hall, Linda Rangell, Ron Ferrando, Henry Lowman, Franklin Peale, and Napoleone Ferrara†

Genentech, Inc., 1 DNA Way, South San Francisco, CA 94080

Contributed by Napoleone Ferrara, January 3, 2007 (sent for review November 28, 2006)

VEGF-A is important in tumor angiogenesis, and a humanized anti-VEGF-A monoclonal antibody (bevacizumab) has been approved by the FDA as a treatment for metastatic colorectal and nonsquamous, non-small-cell lung cancer in combination with chemotherapy. However, contributions of both tumor- and stromal-cell derived VEGF-A to vascularization of human tumors grown in immunodeficient mice hindered direct comparison between the pharmacological effects of anti-VEGF antibodies with different abilities to block host VEGF. Therefore, by gene replacement technology, we engineered mice to express a humanized form of VEGF-A (hum-X VEGF) that is recognized by many anti-VEGF antibodies and has biochemical and biological properties comparable with WT mouse and human VEGF-A. The hum-X VEGF mouse model was then used to compare the activity and safety of a panel of VEGF Mabs with different affinities for VEGF-A. Although *in vitro* studies clearly showed a correlation between binding affinity and potency at blocking endothelial cell proliferation stimulated by VEGF, *in vivo* experiments failed to document any consistent correlation between antibody affinity and the ability to inhibit tumor growth and angiogenesis in most animal models. However, higher-affinity antibodies were more likely to result in glomerulosclerosis during long-term treatment.

angiogenesis | gene knockin | tumor

It is now well established that VEGF-A is an important mediator of physiological and pathological angiogenesis (1). Several VEGF inhibitors have demonstrated efficacy in patients with cancer and neovascular age-related macular degeneration (AMD) (2–7). Among these, the anti-VEGF-A Mab bevacizumab (AVASTIN) has been approved by the FDA for the treatment of metastatic colorectal (8) and nonsquamous, non-small-cell lung cancer (9), in combination with chemotherapy. Bevacizumab is a humanized variant of mouse anti-human VEGF Mab A4.6.1 (10), which was initially identified by its ability to block human VEGF-A-stimulated endothelial cell (EC) proliferation (11) and subsequently was shown to inhibit growth of human tumor xenografts in nude mice (12).

Bevacizumab and Mab A4.6.1 neutralize all isoforms of human VEGF-A and show similar K_d values toward huVEGF-A_{165} (10). Mab Y0317 is an affinity-matured variant of bevacizumab (13). The Fab form of Y0317 (ranibizumab) was recently approved by the FDA for the treatment of neovascular AMD (6).

Although these Mabs block human VEGF-A, they fail to neutralize rodent VEGF-A. Therefore, their main preclinical value has been in disease models in which human VEGF-A is a key driver of angiogenesis (14). However, such antibodies could provide no insight into the role of host-derived VEGF in tumor angiogenesis, nor could they reveal any undesired toxicities associated with VEGF inhibition in rodents (15, 16).

The absence of an anti-VEGF Mab that cross-reacts with murine VEGF-A hindered our efforts to explore therapeutic indications for anti-VEGF antibodies or develop antibodies with improved therapeutic effects relative to the initial Mabs. Although we have recently generated a series of phage-derived Mabs (G6–31, B20–4.1) cross-reactive with rodent and human VEGF-A (17, 18), the differences in species-selectivity between initial and later-generation anti-VEGF antibodies did not allow for a complete comparison of their pharmacological and/or pharmacokinetic properties in WT rodents.

To overcome these limitations, we sought to develop mice expressing a humanized form of VEGF-A. Even modest variations in VEGF expression levels during development may lead to severe tissue damage or lethality (19–22). To avoid such gene dosage effects, we used a gene-replacement technique (gene knockin technology) by which the mouse sequence was replaced with the human counterpart at the corresponding genomic location. Several *in vitro* and *in vivo* studies have indicated that there is little, if any, species-specificity in the effects of VEGF (reviewed in ref. 1). Thus, we hypothesized that adult knockin mice expressing a humanized form of VEGF-A would be viable and could be used as a model to evaluate additional anti-VEGF antibodies with different epitopes and binding affinities, in either immunocompetent or immunodeficient genetic backgrounds. Such a model might be useful also to probe the role of VEGF-A in genetic cancer models in transgenic mice.

Results

Selection of Amino Acids to Be Mutated from Mouse to Human. X-ray structure, combined with site-directed mutagenesis, identified three different regions corresponding to sequences encoded by exons 3 and 4 of VEGF-A that are in direct contact with bevacizumab. The majority of these contacts are formed by residues of the $\beta5$–$\beta6$ loop (around residue 80), with two additional residues from the N-terminal helix and two residues from the $\alpha1$–$\beta2$ loop (around residue 40) interacting at the margin of the interface (23, 24). With the exception of one residue, all of the amino acids of human VEGF-A that are in contact with bevacizumab are conserved in mouse VEGF-A. The nonconserved residue, human Gly-88, corresponds to

Author contributions: H.-P.G. and X.W. contributed equally to this work; H.-P.G., L.D., H.L., and N.F. designed research; H.-P.G., X.W., L.Y., C.W., X.H.L., C.V.L., G.F., C.O., L.D., D.X., J.G., R.C., B.L., L.H., L.R., R.F., and F.P. performed research; X.W., L.Y., C.W., G.F., C.O., D.X., Y.G.M., H.L., and F.P. analyzed data; and N.F. wrote the paper.

Conflict of interest statement: The manuscript describes the use of several anti-VEGF antibodies, including bevacizumab. The authors are employees of Genentech, Inc., the manufacturer of bevacizumab.

Abbreviations: AMD, age-related macular degeneration; EC, endothelial cell.

*Present address: Seattle Genetics, Inc., Bothell, WA 98021.

†To whom correspondence should be addressed. E-mail: nf@gene.com.

This article contains supporting information online at www.pnas.org/cgi/content/full/0611492104/DC1.

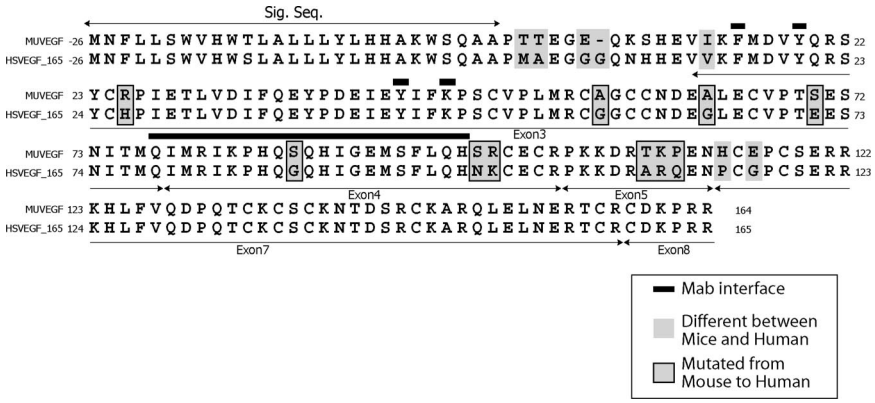

Fig. 1. Ten amino acids mutated from mouse to human to generate the hum-X VEGF variant. Sequence comparison between mouse and human VEGF-A. A total of 19 aa are different between murine $VEGF_{164}$ and human $VEGF_{165}$ (shaded gray). Ten amino acids (boxed and gray) located within exons 3, 4, and 5 of mouse VEGF were mutated to human residues by site-directed mutagenesis.

Ser-87 in the mouse VEGF sequence and is located in the core of the protein–antibody interface. The crystal structure of human VEGF-A in complex with the bevacizumab-Fab revealed that the interface between the molecules is tightly packed [area shown in green, supporting information (SI) Fig. 5*A*]. Modeling of the serine side chain present in mouse VEGF-A, reveals that there is not enough room to accommodate the two additional nonhydrogen atoms that are introduced by the Gly-88→Ser exchange (SI Fig. 5*B*). Previous studies demonstrated that mutation of Gly-88 to alanine (Gly88Ala) in human VEGF-A substantially reduced the binding of Mab A4.6.1 (24). These observations suggested that introducing a single mutation Ser87Gly in mouse VEGF might be sufficient to restore binding to and neutralization by A4.6.1. However, the crystal structure of the complex and the mutagenesis analysis were performed by using a truncated VEGF-A variant (8-109) (24). Therefore, the contribution of residues not present in $VEGF_{8\text{-}109}$ was unknown. Furthermore, phage derived antibodies such as G6-31 or B20-4 were known to contact additional nonconserved residues (area shown in blue, SI Fig. 5 *C* and *D* and ref. 17). These observations prompted us to design a more extensively humanized murine VEGF-A that could be recognized by additional antibodies. We therefore generated two versions of "humanized" VEGF-A proteins. One mutant containing the single Ser87Gly mutation (data not shown) and a second form, hum-X VEGF, in which the 10 residues that are different in the receptor-binding domain between murine and human VEGF-A are replaced by the respective amino acids in the human sequence (Fig. 1).

Characterization of hum-X VEGF Protein and Establishment of hum-X VEGF Knockin (KI) Mice. Recombinant hum-X VEGF, WT human and murine VEGF-A proteins were expressed in *Escherichia coli* and purified (see *SI Text*). We first determined the relative affinities of bevacizumab and three second-generation anti-human VEGF antibodies for the native human VEGF-A and the hum X VEGF protein (SI Table 1). As we hypothesized, the substitution of 10 human amino acids into the murine VEGF-A results in a protein that is recognized by all anti-human VEGF-A Mabs, with little change in affinity relative to WT human VEGF-A. Next, we assessed the potencies of each VEGF-A variant to stimulate proliferation of cultured EC. HuVEGF-A, muVEGF-A, and hum-X VEGF stimulated bovine capillary EC proliferation at half-maximal concentrations of 1.5, 0.6, and 0.9 ng/ml, respectively. Similar results were obtained with HUVE cells (data not shown). Finally, we compared the potencies of the various anti-VEGF-A antibodies to interfere with EC proliferation induced by the various recombinant VEGF-A proteins. As expected, bevacizumab and Y0317 failed to block murine VEGF-A, whereas the EC_{50} values of the remaining ligand/antibody pairs correlated well with antibody affinities, with the exception of B20-4.1, which showed higher than expected EC_{50} toward murine VEGF-A (SI Table 2). These data confirm that the hum-X, WT human, and WT mouse VEGF-A proteins have comparable biological and biochemical properties and that the ability of antibodies to interfere with the hum-X variant relative to WT human VEGF-A correlates with their respective affinities for the WT human protein.

Having established the near equivalency of hum-X VEGF and WT murine VEGF-A *in vitro*, we proceeded to generate gene-targeting vectors to introduce 1 or 10 human amino acids into the mouse germ-line (*SI Text* and SI Fig. 6). Correct recombination events in ES cells were verified by Southern blotting experiments, genomic PCR, and genomic sequencing and by determination of VEGF-A expression in targeted ES cells by ELISA (data not shown). Genotype frequency analysis of >500 KI mice revealed the expected Mendelian ratios of homozygous single mutant or 10-amino acid mutant (hum-X VEGF) mice, and no change in viability and survival of adult mice during a 1 year observation period was found (data not shown). Based on the normal development and viability of both strains, we decided to conduct all further experiments in the more extensively humanized hum-X VEGF KI mice.

Pharmacokinetic and Pharmacodynamic Properties of anti-VEGF-A Antibodies in hum-X VEGF KI Mice. We compared the clearance of bevacizumab, Y0317, and hG6–31 after a single i.v. administration in homozygous hum-X VEGF KI mice and WT (hum-X VEGF WT) control littermates. The systemic clearance of bevacizumab in hum-X VEGF KI mice was ≈3-fold faster than what was observed in hum-X VEGF WT control littermates. In addition, clearance of both higher affinity Mabs (Y0317, G6–31) was ≈3-fold increased relative to bevacizumab in hum-X VEGF KI mice. However, the clearance of G6-31 was similar between WT and hum-X VEGF KI mice, consistent with it's being cross-reactive for both species. In contrast to the affinity-correlated clearance rates observed after a single antibody dose, biweekly administration of antibody for 2–10 weeks was associated with comparable levels of circulating antibodies in serum, but we found no correlation between antibody epitope or affinity. We hypothesize that the discrepancy in the antibody serum levels between single and multiple dose experiments may be due to the rapid binding of higher affinity Mabs to cell surface or extracellular matrix-bound VEGF-A, acting as a sink, and that such mechanism is saturable upon repeat dosing.

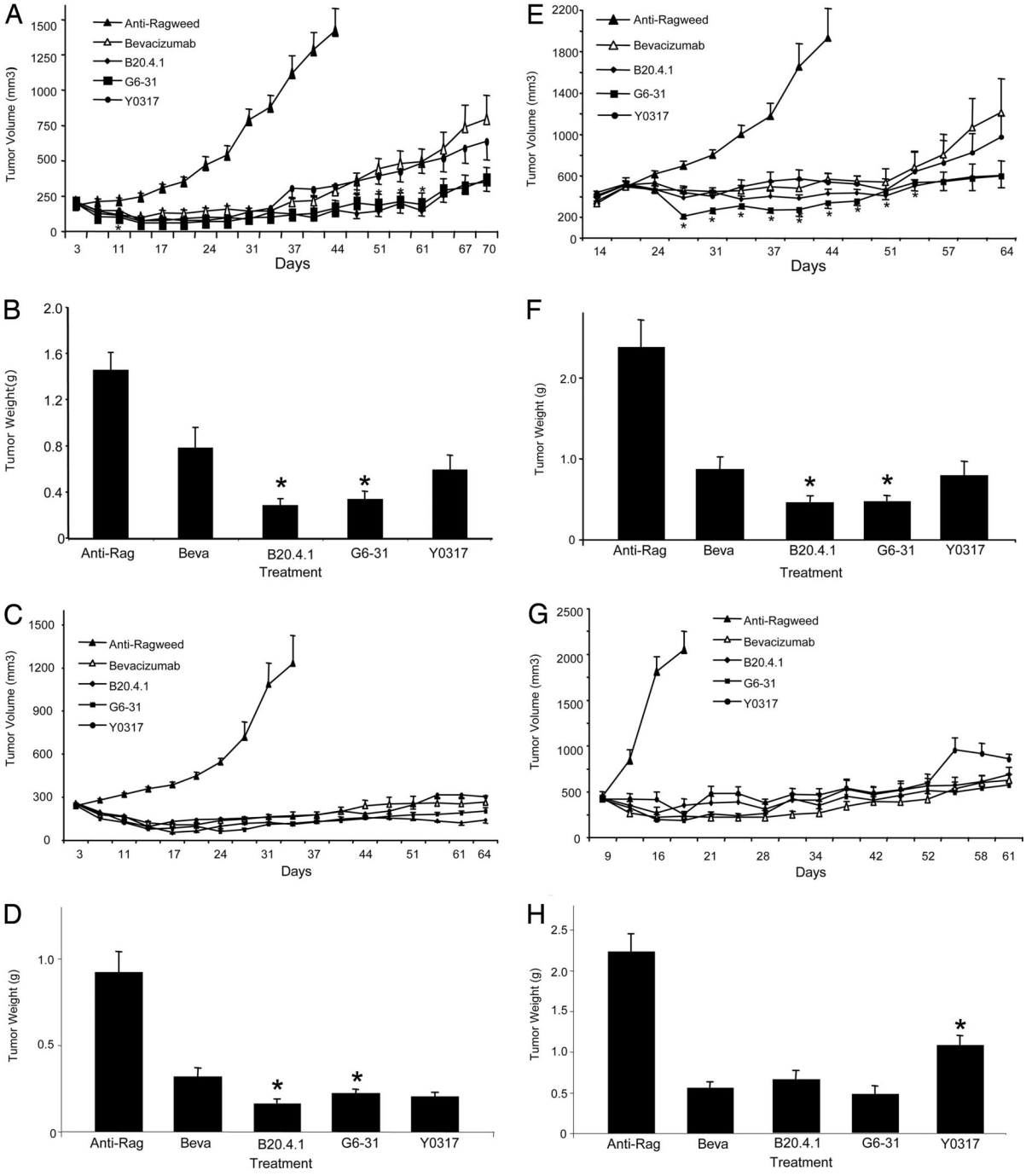

Fig. 2. Efficacy of anti-VEGF-A Mabs in human tumor xenografts implanted s.c. into RAG2 KO; hum-X VEGF KI double-homozygous mice. (*A–D*) Prevention studies. (*E–H*) Intervention studies. (*A*) Growth curves of Calu-6 tumors. Control anti-Ragweed (Anti-Rag), B20–4.1, G6–31, bevacizumab (Beva) or Y0317 Mabs were administered at 5 mg/kg, i.p., twice weekly. (*B*). Terminal weights of Calu-6 tumors from experiment in *A* at day 70 of treatment. Control animals were killed at day 44. Tumors from B20-4.1- and G6-31-treated animals had significantly lower weight than the bevacizumab group. (*C*) Growth curves of human HT29 colorectal carcinoma cells. (*D*) Terminal weights of HT29 tumors from the experiment in *C* as determined at day 67. Controls were killed at day 33. (*E*) Growth curves of Calu-6 tumors in which treatment was initiated after tumor volumes reached ≈400 mm^3 (regression study). (*F*) Terminal tumor weights of Calu-6 tumors in *E* were determined at day 63. Controls were harvested at day 42. (*G*) Growth curves of human HM7 colorectal tumor. Similar to *E* and *F*, antibody treatment was initiated after tumor volumes reached ≈400 mm^3. (*H*) Terminal weights of HM7 tumors determined on day 61. Controls were killed at day 19. Data shown are Means ± SEM. *, Significant difference ($P < 0.05$) compared with the bevacizumab group.

Immunocompromised RAG2 KO; hum-X VEGF KI double-homozygous mice were bred and used to assess the potency and efficacy of bevacizumab, hY0317, hG6-31 and hB20-4.1 to inhibit growth of Calu-6 (lung carcinoma), HT29 or HM7 (colorectal carcinoma) tumor xenografts. As shown in Fig. 2, when given at the dose of 5 mg/kg twice weekly, bevacizumab and hY0317 interfered to similar extents with growth of human Calu-6 lung carcinoma tumors, despite marked differences in their relative binding affinities for VEGF-A. Similarly, B20-4.1 and G6-31 were equally efficacious at inhibiting growth of Calu-6 lung carcinoma cells (Fig. 2 *A* and *B*). A similar response was observed when antibodies were tested in HT-29 tumors (Fig. 2 *C* and *D*).

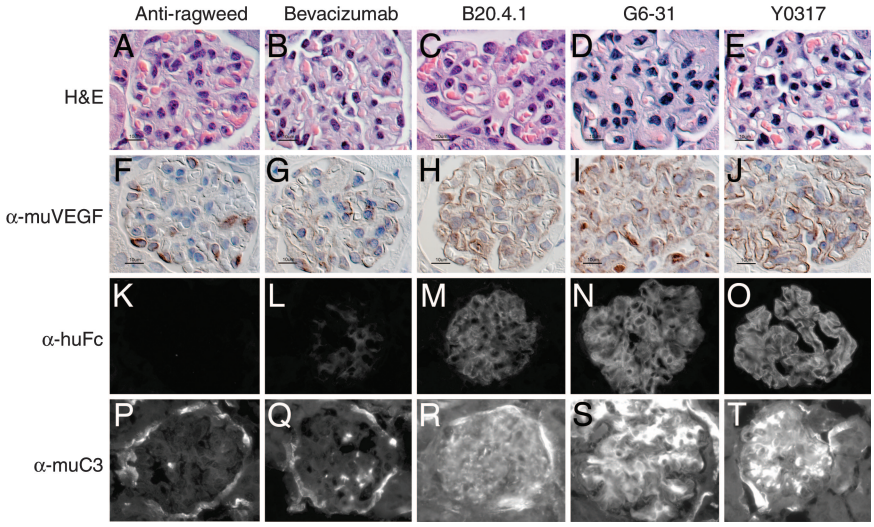

Fig. 3. Renal changes in homozygous RAG2 KO; hum-X VEGF KI double-homozygous mice treated with anti-VEGF-A antibodies (human Fc framework). Animals treated (5 mg/kg, two times weekly for 54 days) with antibodies having increasing affinity for VEGF-A have increased glomerulosclerosis with expanded mesangial areas and thickened capillary loops (*A–E*). Anti-murine VEGF staining (*F–J*); control animals (*F*) show moderate podocyte-specific staining, without capillary loop or mesangial signal; treatment with antibodies of increasing affinity (*G–J*) results in progressively increased signal in mesangial areas and capillary loops; capillary loop staining in variably linear (*J*, Y0317) or more coarsely granular (*I*, G6–31). VEGF-A signal in juxtamedullary glomeruli is consistently stronger than in peripheral cortical glomeruli (detail not shown). Anti-human Fc (*K–O*, direct immunofluorescence); anti-VEGF antibodies of increasing affinity accumulate in glomeruli roughly in proportion to their affinity. Complement C3 (*P–T*, direct immunofluorescence); anti-VEGF antibodies of increasing affinity result in complement C3 deposition in glomeruli, roughly in proportion to their affinity; nonspecific signal is present in Bowman's capsule basement membrane surrounding glomerular tuft.

In the majority of prevention experiments, we noted a small but reproducible trend toward improved tumor growth inhibition by B20-4.1 or G6-31 Mabs relative to bevacizumab or Y0317 (Fig. 2 *A–D* and data not shown). Interestingly, even when tested at a 10-fold-lower dose (0.5 mg/kg twice weekly), the higher-affinity Mabs did not show any clear advantage relative to the lower-affinity Mabs (SI Fig. 7 and data not shown). Finally, we tested the ability of anti-VEGF-A antibodies to affect growth of established tumors. For this purpose, we administered bevacizumab, Y0317, B20-4.1, and G6-31 to mice implanted with Calu-6 (Fig. 2 *E* and *F*) or HM7 tumors (Fig. 2 *G* and *H*) when tumor reached an average size of 400–500 mm^3. All antibodies suppressed tumor growth. However, similar to the prevention experiments, there was a very modest trend toward increased efficacy of Mabs B20-4.1 and G6-31, at least in the Calu-6 model (Fig. 2 *E* and *F*).

Long-Term Toxicity of anti-VEGF-A Antibodies Is Related to Binding Affinity. We treated hum-X VEGF-KI mice when reaching 3, 6, or 9 months of age for prolonged periods of time. Antibodies were administered at low (5 mg/kg, i.p., once weekly) or high doses (10 mg/kg, i.p., twice weekly) for 12 consecutive weeks. Treatment with higher-affinity Mabs was frequently associated with the formation of ascites, which was dose-dependent. The effect was seen infrequently at doses of ≤5 mg/kg weekly but was frequent at higher doses. In contrast, administration of the lower-affinity A4.6.1 or mB20-4.1 Mabs did not result in ascites formation. Serum chemistry and urine analysis on days 84–90 (A4.6.1, B20-4.1, G6-31) or when animals became moribund (Y0317) revealed increased alanine aminotransferase (ALT), aspartate aminotransferase (AST), and blood urea nitrogen levels, consistent with liver and kidney injury (data not shown).

Histological analysis of all major organs identified no significant changes in heart, spleen, pancreas, and lung in any treatment group. However, there were subtle changes in the liver and more significant changes in kidney, both of which were most prominent in mice treated with higher-affinity anti-VEGF Mabs for long durations. In animals treated with anti-VEGF antibodies, H&E-stained liver samples showed increased numbers of mononuclear cells adherent to central veins, whereas portal veins appeared normal. The adherent cells were F4/80- and MAC-2-positive, consistent with macrophages of Kupffer cells; some contained phagocytosed red blood cells. Increased VEGF-A staining was present in sinusoidal EC (SI Fig. 8). By direct immunofluorescence, no detectable anti-VEGF antibody or complement C3 deposition was noted in frozen samples of the same liver samples (data not shown).

Kidneys of animals treated for extended periods with anti-VEGF Mabs showed glomerulosclerosis, which was generally more severe in animals treated with high-affinity Mabs (Fig. 3). Glomeruli in the most affected animals showed severe diffuse global sclerosis. Immunostaining for murine VEGF-A showed marked differences between control and anti-VEGF-treated animals: control glomeruli showed moderate signal in podocyte cell bodies, with little detectable signal in capillary loops. In contrast, anti-VEGF-treated glomeruli showed increased mesangial and capillary loop staining, roughly in proportion to the affinity of the respective antibodies. In addition, juxtamedullary glomeruli showed more intense and widespread staining than the corresponding peripheral cortical glomeruli in the same animal. Anti-human Fc direct immunofluorescence showed increased anti-VEGF deposition (diffuse, finely granular pattern) in glomeruli, which was more prominent with antibodies of increased affinity. Similarly, complement C3 staining was increasingly prominent in animals treated with higher-affinity anti-VEGF antibodies. MAC-2 immunohistochemistry showed no significant infiltration of monocytes/macrophages in glomeruli from anti-VEGF-treated animals (data not shown). Toluidine blue and silver staining of methacrylate-embedded 1-μm sections (Fig. 4) confirmed the observations from paraffin and frozen sections, showing increased mesangial cellularity and widening of mesangial matrix and capillary loops with material that stained differently from native basement membrane. Electron-microscopic examination (Fig. 4) showed focal subendothelial

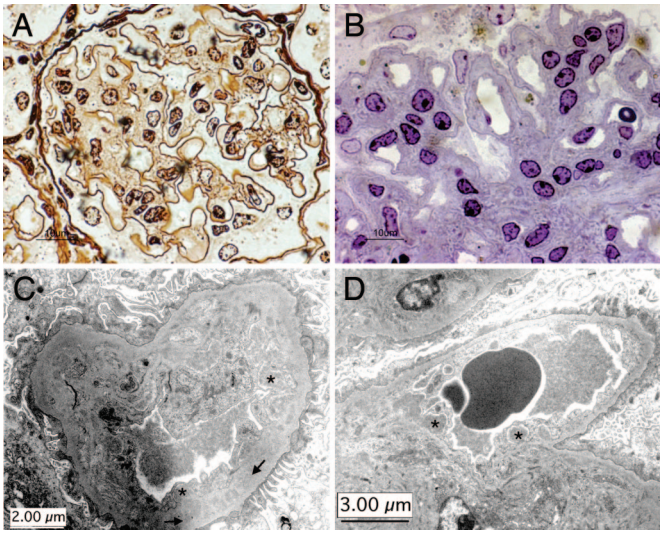

Fig. 4. Renal ultrastructural changes in homozygous RAG2 KO; hum-X VEGF KI double-homozygous mice treated with anti-VEGF-A antibodies (murine Fc framework). (*A* and *B*) Treatment with G6–31 5 mg/kg, weekly for 8 weeks, results in diffusely increased mesangial cellularity, widening of mesangium and capillary loops by amorphous extracellular material (1-μm methacrylate sections; Jones silver stain (*A*) and toluidine blue (*B*). (*C* and *D*) Treatment with G6–31 10 mg/kg, twice weekly for 8 weeks, results in variably distorted EC, focally enveloping amorphous subendothelial deposits (asterisks indicate presumably immune complexes); EC frequently lack regularly spaced fenestrations. Basement membrane shows focal reduplication (arrows). Podocyte foot processes are variably fused.

deposits in capillary loops, endothelial swelling, and increased mesangial matrix and mesangial cell number. In contrast, podocyte foot processes were relatively spared, although focal foot-process fusion was evident in the more severely affected glomeruli. Together, these observations are consistent with the presence of VEGF–anti-VEGF complexes deposited in the glomeruli.

Discussion

Given the fact that VEGF-A represents a clinically validated therapeutic target in cancer and other diseases (2–7), we wished to define more clearly the physicochemical parameters of anti-VEGF-A antibodies that affect their therapeutic potency and efficacy. Even though *in vitro* studies demonstrated a correlation between antibody-binding affinity and potency in assays measuring inhibition of VEGF-stimulated EC proliferation (SI Table 2), various affinity-matured anti-VEGF-A antibodies *in vivo* did not show in most models a clearly increased potency or efficacy (Fig. 2 and SI Fig. 7) to block tumor growth, when compared with their lower-affinity counterparts. How can we explain such apparent discrepancy? Anti-VEGF-A antibodies are expected to interfere with angiogenesis primarily by preventing VEGF-A from binding to its receptors in the tumor vasculature. Thus, in contrast to Mabs that directly target antigens in the tumor cells, anti-VEGF-A antibodies may not need to penetrate the tumor mass to induce pharmacologic effects. Therefore, it is possible that inhibition of VEGF-A binding to VEGFRs can be saturated when lower-affinity anti-VEGF-A antibodies are used. In this context, it is interesting that previous studies with antiviral antibodies showed that the *in vitro* neutralization abilities correlated well with avidity and affinity. However, *in vivo* protection was independent of antibody avidity and affinity, above a threshold value, and depended essentially on achieving a minimum serum concentration (25).

Based on the observation that VEGF RTK inhibitors have greater antitumor efficacy when the treatment is initiated at early stages of tumor progression in certain models (26, 27), it has been suggested that alternative angiogenic factors are produced progressively during advanced stages of tumorigenesis, rendering late-stage tumors relatively insensitive to such therapy. However, administration of either lower- or higher-affinity anti-VEGF Mabs to mice bearing already established HM-7 or Calu-6 tumors suppressed tumor growth over prolonged periods of time, and treatment with bevacizumab was frequently associated with tumor regression, at least initially (Fig. 2 *E–H*). These findings emphasize the importance of VEGF-A in all stages of tumor angiogenesis.

After single-bolus administration in hum-X VEGF KI mice, higher-affinity Mabs appeared to be cleared more rapidly from the circulation when compared with their lower-affinity counterparts (data not shown) However, no clear correlation between antibody affinity or epitope binding and clearance was found in repeat-dosing experiments. One potential mechanism that may contribute to serum clearance after single-dose administration may be the increased potential of higher-affinity Mabs to be retained by membrane-bound host VEGF-A, leading to more rapid depletion of higher-affinity Mabs from the circulation.

Binding of an epitope that overlaps more closely with the receptor-binding sites on VEGF-A appeared to be associated with a modest trend toward improved efficacy, which achieved statistical significance in some cases. However, considering that anti-VEGF therapy is usually done in combination with cytotoxic chemotherapy and/or other anticancer agents (4, 28, 29), the relative clinical efficacy of those therapeutic regimens remains to be determined. In contrast, increasing antibody affinity did not affect efficacy or potency in most models, but resulted in increased toxicity, including glomerulosclerosis, hypoalbuminemia, and ascites formation. Hypoproteinemia secondary to glomerular damage clearly correlates with ascites; it is unclear whether decreased hepatic protein synthesis and/or increased portal venous pressure also contribute. Increased toxicity in hum-X VEGF KI mice appears to be an on-target effect, because antibodies with higher affinities (Y0317, G6–31) derived from different parental clones, and soluble VEGF receptors induce similar pathophysiological changes (data not shown). The development of ascites may seem superficially paradoxical, considering that VEGF inhibition may reduce ascites formation in models of ovarian carcinoma (30, 31). However, VEGF blockade achieved by high-affinity soluble VEGFR-1 has been previously reported to result in ascites formation, liver injury, and increased lethality in mice (32, 33). The increase in VEGF-A staining in affected organs such as liver and kidney, combined with the significant amounts of serum VEGF-A bound to higher-affinity antibodies, suggest that compensatory up-regulation in response to interference with physiologic maintenance functions of VEGF-A may occur. In other reports, treatment of adult mice with various VEGF inhibitors resulted in a significant reduction in the density of capillaries in several organs (34, 35). Such effects were most prominent in young mice (34). Although it is unknown to what degree tonic VEGF-A levels are important for tissue homeostasis in adults, our findings indicate that a very tight VEGF-A neutralization is prone to induce a prolonged vascular damage. In contrast, a less-tight neutralization appears to be associated with a lower degree of toxicity, even though it may result in a comparable suppression of tumor angiogenesis. One of the possibilities is that pools of VEGF-A particularly important for vascular maintenance are not readily accessible to inhibitors (e.g., extracellular matrix-bound VEGF) and thus require a particularly stringent blockade to be neutralized. It is noteworthy that VEGF neutralization may be associated with an increase in hepatic erythropoietin synthesis but only after a very tight blockade (36).

Interestingly, we identified increased complement deposition in kidneys of mice treated with higher-affinity relative to lower-affinity anti-VEGF-A Mabs. Therefore, it is conceivable that Fc effector functions of high-affinity antibodies localized to kidney glomeruli may contribute to the pathology associated with glomer-

ulosclerosis. However, VEGF inhibitors that lack effector functions have been also associated with kidney damage. (37 38).

We cannot rule out the possibility that modifications in VEGF inhibitors different from those described in the present studies may yield different results. However, it is intriguing that the VEGF-Trap, a VEGF blocker selected for its high binding affinity (39), has demonstrated dose-limiting toxicities in humans, including proteinuria, leading to discontinuation of clinical trials testing the i.v. administration of this agent in AMD patients (reviewed in ref. 40). On the other hand, our findings do not exclude the possibility that high binding affinity may provide an advantage in circumstances in which there is little or no systemic exposure. High-affinity VEGF-A binding might be helpful to achieve a complete VEGF neutralization when the ratio inhibitor/VEGF is low, for example in local or regional therapies.

Materials and Methods

Reagents. Recombinant murine VEGF-A and murine and human VEGFR1 and VEGFR2 proteins were purchased from R & D Systems (Minneapolis, MN). Recombinant human VEGF-A (165 amino acid isoforms) was purified from *E. coli*. [^{125}I]VEGF-A was purchased from Amersham (Piscataway, NJ).

The Y0317 lineage was previously described (13). G6-31 and B20-4.1 Mabs were derived from human(ized) Fab phage libraries as described (18). Full-length human antibodies (hY0317, etc.) were generated by grafting the variable heavy (VH) and variable light (VL) domains from these Fabs onto the constant domains of human IgG1(κ). For long-term administration in immunocompetent mice or for control experiments, full-length reverse-chimeric murine antibodies were generated by grafting the VH and VL variable domains onto the constant domains of murine IgG2a (κ). Mouse anti-Ragweed Mab (control Mab) belonged to the IgG2a isotype.

Tumor Implantation and *in Vivo* Treatments. Human HT29 (colorectal carcinoma) and Calu-6 (lung carcinoma) cells were obtained from the American Type Culture Collection (Manassas, VA). The human colorectal carcinoma HM-7 cell line is a derivative of LS 174T (41). Tumor cells were maintained in culture with DMEM/F12 medium, supplemented with 10% FBS. Cells were grown at 37°C in 5% CO_2 until confluent, harvested, and resuspended in sterile Matrigel at 25×10^6 cells per ml. Xenografts were established in 6- to 8-week-old female Beige Nude XID mice by dorsal flank s.c. injection of 5×10^6 cells per mouse and allowed to grow. In prevention studies, the treatment with antibodies was initiated 48 h after tumor cell inoculation. For intervention studies, when tumors reached a volume of $\approx$400 mm^3, a cohort was randomly selected ($n = 10$) as day-0 controls. The remaining mice were divided into groups of 10 mice, and antibodies were administered i.p. at the dose of 5 mg/kg twice weekly. The transplanted tumors were measured twice weekly along the longest axis and the perpendicular axis as described (15). For each day on which tumors were measured, the tumor volume for each mouse was calculated, and the tumor volume means from each noncontrol, nonbevacizumab group were compared with the tumor volume mean of bevacizumab-treated mice by Dunnett's *t* test (42) implemented in the JMPTM Statistical Analysis System (version 5.1 for Windows; SAS Institute, Cary, NC), at a level of $P < 0.05$. Mice were killed when tumor volume reached $\approx$2,000 mm^3.

We thank William Forrest for help in statistical analysis and Farbod Shojaei for reading the manuscript.

1. Ferrara N (2004) *Endocr Rev* 25:581–611.
2. Ferrara N, Hillan KJ, Gerber HP, Novotny W (2004) *Nat Rev Drug Discov* 3:391–400.
3. Gasparini G, Longo R, Toi M, Ferrara N (2005) *Nat Clin Pract Oncol* 2:562–577.
4. Ferrara N, Kerbel RS (2005) *Nature* 438:967–974.
5. Jain RK, Duda DG, Clark JW, Loeffler JS (2006) *Nat Clin Pract Oncol* 3:24–40.
6. Ferrara N, Damico L, Shams N, Lowman H, Kim R (2006) *Retina* 26:859–870.
7. Ng EW, Sima DT, Calias P, Cunningham ET, Jr, Guyer DR, Adamis AP (2006) *Nat Rev Drug Discov* 5:123–132.
8. Hurwitz H, Fehrenbacher L, Novotny W, Cartwright T, Hainsworth H, Helm W, Berlin J, Baron A, Griffing S, Holmgren E, *et al.* (2004) *N Engl J Med* 350:2335–2342.
9. Sandler A, Gray R, Perry MC, Brahmer J, Schiller JH, Dowlati A, Lilenbaum R, Johnson DH (2006) *N Engl J Med* 355:2542–2550.
10. Presta LG, Chen H, O'Connor SJ, Chisholm V, Meng YG, Krummen L, Winkler M, Ferrara N (1997) *Cancer Res* 57:4593–4599.
11. Kim KJ, Li B, Houck K, Winer J, Ferrara N (1992) *Growth Factors* 7:53–64.
12. Kim KJ, Li B, Winer J, Armanini M, Gillett N, Phillips HS, Ferrara N (1993) *Nature* 362:841–844.
13. Chen Y, Wiesmann C, Fuh G, Li B, Christinger HW, McKay P, de Vos AM, Lowman HB (1999) *J Mol Biol* 293:865–881.
14. Gerber HP, Ferrara N (2005) *Cancer Res* 65:671–680.
15. Gerber HP, Kowalski J, Sherman D, Eberhard DA, Ferrara N (2000) *Cancer Res* 60:6253–6258.
16. Tejada M, Yu L, Dong J, Jung K, Meng G, Peale FV, Frantz GD, Hall L, Liang X, Gerber HP, Ferrara N (2006) *Clin Cancer Res* 12:2676–2688.
17. Fuh G, Wu P, Liang WC, Ultsch M, Lee CV, Moffat B, Wiesmann C (2006) *J Biol Chem* 281:6625–6631.
18. Liang WC, Wu X, Peale FV, Lee CV, Meng YG, Gutierrez J, Fu L, Malik AK, Gerber HP, Ferrara N, Fuh G (2006) *J Biol Chem* 281:951–961.
19. Ferrara N, Carver Moore K, Chen H, Dowd M, Lu L, O'Shea KS, Powell Braxton L, Hillan KJ, Moore MW (1996) *Nature* 380:439–442.
20. Gerber HP, Hillan KJ, Ryan AM, Kowalski J, Keller, G-A, Rangell L, Wright BD, Radtke F, Aguet M, Ferrara N (1999) *Development (Cambridge, UK)* 126:1149–1159.
21. Miquerol L, Langille BL, Nagy A (2000) *Development (Cambridge, UK)* 127:3941–3946.
22. Baluk P, Lee CG, Link H, Ator E, Haskell A, Elias JA, McDonald DM (2004) *Am J Pathol* 165:1071–1085.
23. Muller YA, Li B, Christinger HW, Wells JA, Cunningham BC, de Vos AM (1997) *Proc Natl Acad Sci USA* 94:7192–7197.
24. Muller YA, Chen Y, Christinger HW, Li B, Cunningham BC, Lowman HB, de Vos AM (1998) *Structure (London)* 6:1153–1167.
25. Bachmann MF, Kalinke U, Althage A, Freer G, Burkhart C, Roost H, Aguet M, Hengartner H, Zinkernagel RM (1997) *Science* 276:2024–2027.
26. Casanovas O, Hicklin DJ, Bergers G, Hanahan D (2005) *Cancer Cell* 8:299–309.
27. Bergers G, Song S, Meyer-Morse N, Bergsland E, Hanahan D (2003) *J Clin Invest* 111:1287–1295.
28. Jain RK (2005) *Science* 307:58–62.
29. Kerbel RS (2006) *Science* 312:1171–1175.
30. Luo JC, Toyoda M, Shibuya M (1998) *Cancer Res* 58:2594–2600.
31. Hu L, Hofmann J, Zaloudek C, Ferrara N, Hamilton T, Jaffe RB (2002) *Am J Pathol* 161:1917–1924.
32. Kuo CJ, Farnebo F, Yu EY, Christofferson R, Swearigen RA, Carter R, von Recum HA, Yuan J, Kumihara J, Flynn E, *et al.* (2001) *Proc Natl Acad Sci USA* 98:4605–4610.
33. Mahasreshti PJ, Kataram M, Wang MH, Stockard CR, Grizzle WE, Carey D, Siegal GP, Haisma HJ, Alvarez RD, Curiel DT (2003) *Clin Cancer Res* 9:2701–2710.
34. Baffert F, Le T, Sennino B, Thurston G, Kuo CJ, Hu-Lowe D, McDonald DM (2006) *Am J Physiol* 290:H547–H559.
35. Kamba T, Tam BY, Hashizume H, Haskell A, Sennino B, Mancuso MR, Norberg SM, O'Brien SM, Davis RB, Gowen LC, *et al.* (2006) *Am J Physiol* 290:H560–H576.
36. Tam BY, Wei K, Rudge JS, Hoffman J, Holash J, Park SK, Yuan J, Hefner C, Chartier C, Lee JS, *et al.* (2006) *Nat Med* 12:793–800.
37. Maynard SE, Min JY, Merchan J, Lim KH, Li J, Mondal S, Libermann TA, Morgan JP, Sellke FW, Stillman IE, *et al.* (2003) *J Clin Invest* 111:649–658.
38. Hara A, Wada T, Furuichi K, Sakai N, Kawachi H, Shimizu F, Shibuya M, Matsushima K, Yokoyama H, Egashira K, Kaneko S (2006) *Kidney Int* 69:1986–1995.
39. Holash J, Davis S, Papadopoulos N, Croll SD, Ho L, Russell M, Boland P, Leidich R, Hylton D, Burova E, *et al.* (2002) *Proc Natl Acad Sci USA* 99:11393–11398.
40. Michels S, Schmidt-Erfurth U, Rosenfeld PJ (2006) *Expert Opin Investig Drugs* 15:779–793.
41. Warren RS, Yuan H, Matli MR, Gillett NA, Ferrara N (1995) *J Clin Invest* 95:1789–1797.
42. Dunnett CW (1955) *J Am Stat Assoc* 50:1096–1121.